Nonelastic Scattering Cross Sections for Fast Neutrons*†

H. L. TAYLOR, O. LÖNSJÖ, AND T. W. BONNER
The Rice Institute, Houston, Texas

(Received June 16, 1955)

Measurements have been made of the nonelastic cross sections of neutrons in Be, C, Al, Ti, Cr, Fe, Ni, Cu, Ag, Sn, Pb, and Bi. These cross sections include all processes except elastic scattering. The experiments have been carried out with monoenergetic neutrons of 3.5, 4.7, 7.1, 12.7, and 14.1 Mev. The neutrons were produced with a Van de Graaff accelerator using the nuclear reactions: $T^3(p,n)He^3$, $D(d,n)He^3$, and $T^3(d,n)He^4$. Cross sections were determined from transmissions through spherical shells which were 3.8 cm in radius and 2 cm thick. A new type of neutron detector which gives energy information about neutrons and is insensitive to γ radiation was placed at the center of the spherical shell and was used as a biased detector of neutrons. The results of these experiments show that the nonelastic neutron cross section for 12.7- and 14.1-Mev neutrons is nearly geometrical and is closely approximated by $\sigma=\pi(R+\lambda\!\!\!^{-})^2$, where $R=1.4\times10^{-13}A^{\frac{1}{3}}$. The nonelastic cross sections are roughly constant in the energy range 5 to 14 Mev; below about 5 Mev the cross sections begin to decrease.

The elastic cross sections can be obtained by subtracting the nonelastic cross sections from the total cross sections. The variations with energy of the nonelastic and elastic cross sections are quite different.

Data with 12.7-Mev neutrons and low counter bias, give the relative number of γ rays given off per inelastic collision of these neutrons. The number of γ rays decreases rapidly with increasing atomic number and there are less than 5% as many γ rays from Bi as from Al, Ti, Cr, and Fe.

INTRODUCTION

NUMEROUS experiments have been carried out to determine the magnitudes of the total neutron cross sections in various elements. Other experiments have been made to determine the cross sections for the different processes that make up the total cross sections. In the energy range of 3 to 15 Mev, which is to be discussed in this paper, the total neutron cross section is largely made up of the elastic, inelastic, and $(n,2n)$ processes. The experimentally measured quantity, however, is the total cross section minus the elastic cross section, which is defined as the nonelastic cross section. With neutrons of high energies the nonelastic cross section is very nearly equal to the reaction cross section. With low-energy neutrons and with intermediate energies where there are only a few possible excited states of the struck nucleus, the nonelastic cross section is less than the reaction cross section by the amount of the compound elastic scattering. Early experiments[1] with a radium-beryllium source of neutrons placed inside a spherical absorber qualitatively measured the cross section for inelastic scattering of neutrons in the absorber. More recent experiments[2,3] with 14-Mev neutrons and threshold detectors gave results which are in general agreement with the present cross sections.

Another method for estimating the inelastic scattering cross section has been to determine the neutron spectrum by the exposure of photographic plates to neutrons.[4,5] Measurements by Graves and Rosen with 14- to 15-Mev neutrons indicate that for all elements from aluminum to bismuth almost all the inelastically scattered neutrons have an energy of less than 5 Mev. This method is good for finding the energy distribution of the inelastically scattered neutrons but is not adapted for accurate quantitative values of the cross section.

If a monoenergetic source of neutrons is surrounded by a sphere of a material with which the neutrons could interact only by elastic scattering, a biased detector, whose energy discrimination was not sufficiently sharp to resolve the small loss of energy from elastic scattering, would count at the same rate with the scatterer on as with the scatterer off. If, however, the neutrons are inelastically scattered with sufficient loss of energy such that they will not be detected, then they have been effectively absorbed in a transmission experiment.

It is more convenient to place the detector inside the spherical scatterer which subtends a small solid angle from a source so that all the neutrons incident on the scatterer have very nearly the same energy. A general proof for the validity of such an interchange of source and detector has been given by Bethe.[6]

The general theory for calculating nonelastic cross sections by transmission through a thick spherical shell has been worked out by Bethe, Beyster, and Carter[7] and has been used in analyzing the experimental results reported herein. The purposes of the present research were to adapt a new scintillation type detector to a useful form and to measure the nonelastic scattering

* Supported in part by the U. S. Atomic Energy Commission.

† Preliminary report of these results was given at the Pittsburgh Conference on Medium Energy Nuclear Physics, June, 1953 (unpublished); Birmingham Conference on Nuclear Physics, July, 1954 (unpublished); and Phys. Rev. **94**, 807(A) (1954).

[1] Dunning, Pegram, Fink, and Mitchell, Phys. Rev. **48**, 265 (1935); Seaborg, Gibson, and Grahame, Phys. Rev. **52**, 408 (1937); D. C. Grahame and G. T. Seaborg, Phys. Rev. **53**, 795 (1938).

[2] Gittings, Barschall, and Everhart, Phys. Rev. **75**, 1610 (1949).

[3] Phillips, Davis, and Graves, Phys. Rev. **88**, 600 (1952).

[4] P. H. Stetson and Clark Goodman, Phys. Rev. **82**, 69 (1951); E. R. Graves and L. Rosen, Phys. Rev. **89**, 343 (1953).

[5] B. G. Whitmore and G. E. Dennis, Phys. Rev. **84**, 296 (1951); B. G. Whitmore, Phys. Rev. **92**, 654 (1953).

[6] H. A. Bethe, Los Alamos Report LA-1428, 1952 (unpublished).

[7] Bethe, Beyster, and Carter, Los Alamos Report LA-1429 (unpublished).

cross sections of elements of various atomic weights as a function of energy from 3.5 to 14.1 Mev.

APPARATUS

The scattering samples were thick spherical shells with a standard size of 7.62 cm outside diameter with a 2 cm wall thickness. There was a hole of 1.62-cm diameter through the shell for the insertion of the light pipe to the counter. The spheres were machined to a tolerance of less than 0.002 cm from commercially available materials. The one exception to the standard size was the chromium sphere which was 7.15 cm in outside diameter with a 2-cm wall.

The neutron detectors were made of an organic scintillator which gave light pulses from recoil protons caused by neutron scattering in the scintillator.[8] The light pulse is proportional to the range of the ionizing particle in the scintillator.[9] In order to count neutrons and not γ rays, it was necessary to make pulses due to Compton electrons a factor of 2 to 3 smaller than the neutron pulses. The plastic scintillator[10] was made into spheres of such size that an electron passing through the diameter of the scintillating sphere would give less than half as large a pulse as neutrons from the source. Anthracene crystals were used in the first experiments. A plastic scintillator was substituted for the anthracene detector since the pulse size in anthracene varies as much as 15% with the direction of the neutrons. The plastic scintillators and the detectors made from them did not show directionality of response.

In order to have a high counting rate it is desirable to use a scintillator with a large volume. For the 12.7- and 14-Mev neutron detector, it would have been possible to use a scintillation sphere 2 cm in diameter and still discriminate against γ-ray pulses. A 1 cm diameter scintillator was used and was large enough to give an adequate counting rate. The maximum pulse due to γ rays in this scintillator is produced by a 2.5-Mev electron which will have a range of 1 cm in the plastic. Such a pulse is the same size as that of a 6-Mev recoil proton.

An adequate counting rate for 7.1-Mev neutrons was obtained with a single sphere with a diameter of 6.5 mm. An electron of 1.6 Mev will just traverse the sphere and produce a pulse in the scintillator equal to half that from a 7-Mev recoil proton.

For the 4.7-Mev neutron detector, it was necessary to use spheres with a diameter of 2.5 mm. The range of a 0.75-Mev electron is 2.5 mm; an electron of this energy produces a pulse 45% as large as a 4.7-Mev recoil proton in the scintillator. A single sphere of 2.5-mm diameter did not give a satisfactory counting rate, so a detector was constructed using four such spheres. Two

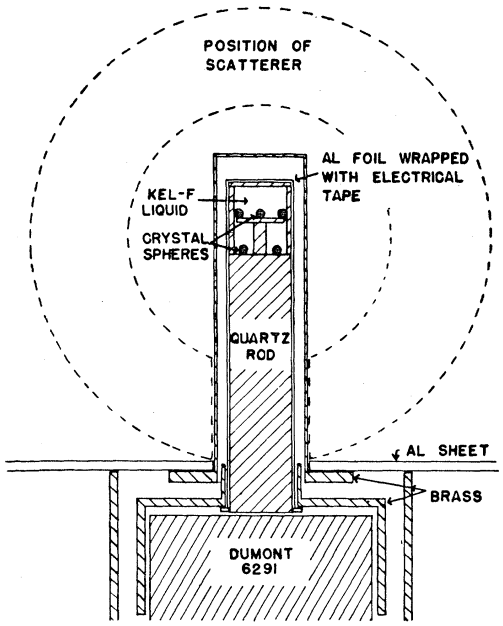

FIG. 1. Diagram of neutron detector showing spherical scintillators, quartz light pipe, and position of the scattering sample.

spheres were placed in each of two layers, the upper layer being supported on a glass disk and positioned so that the spheres were not directly above the spheres in the lower layer. To improve optical coupling and to place electron stopping material between the spheres, the volume of the detector was filled with Kel-F fluid[11] ($Cl_3F_3C_6$). A fluid containing no hydrogen was used to avoid production of recoil protons in the fluid. The minimum energy of an electron which passes through two spheres and the intervening Kel-F is 4 Mev.

The 3.5-Mev neutron detector was constructed of scintillation spheres with a diameter of 1.5 mm. An electron of 0.5 Mev produces a pulse equal to 50 percent of the pulse from a 3.5-Mev proton and has a range of 1.5 mm in the scintillator. Eight spheres were arranged at quadrant points of each of two layers in a glass tube of 10 mm inside diameter. Spheres in the upper layer were supported by a glass disk and were not directly over the spheres of the lower layer. The sealed volume was filled with Kel-F fluid. Only electrons with energies greater than 3 Mev could traverse two spheres and the minimum intervening material. The 3.5-Mev detector and mounting to hold the spherical absorbers is illustrated in Fig. 1. The detectors were constructed on a quartz rod of such a length as to place the geometrical center of the detector at the center of the scattering shell. The detector and quartz were wrapped with 0.0005 inch aluminum foil and scotch electrical tape and optically coupled to the Dumont 6291 photomultiplier tube by silicone vacuum grease.

[8] McCrary, Taylor, and Bonner, Phys. Rev. **94**, 808(A) (1954).
[9] J. B. Birks, Phys. Rev. **84**, 364 (1951); Taylor, Jentschke, Remley, Eby, and Kruger, Phys. Rev. **84**, 1034 (1951).
[10] Obtained from Nuclear Enterprises, Ltd., 1124 Grosvenor Avenue, Winnipeg, Canada.
[11] Manufactured by W. M. Kellogg Company, Chemical Manufacturing Division, Jersey City, New Jersey.

Nuclear reactions induced by particles accelerated in the Rice Institute Van de Graaff accelerator were used as monoenergetic neutron sources. To minimize background effects of neutrons scattered from matter near the source, a minimum amount of material was used at the end of the vacuum tube for the target mounting, and cooling of the target was accomplished by compressed air. The target and the counting apparatus were over a pit which was eight feet deep and covered by a one-quarter inch aluminum floor.

Neutrons of 3.5 Mev were produced by 4.2-Mev protons from the $T(p,n)He^3$ reaction at zero degrees to the incident beam. The target was tritium adsorbed in a zirconium layer which had been evaporated onto a tungsten blank. The particular target used was obtained from Oak Ridge National Laboratories and had a zirconium layer of 1 mg/cm^2. The angular distribution of the $T(p,n)He^3$ reaction has been measured[12] and the change of energy of the neutrons with angle of emission can be calculated. The detector was four and a half inches from the source, giving a 110-kev decrease in energy at the outer edge of the shell and 10% illumination decrease at the outer edge of the shell.

The $D(d,n)He^3$ reaction was used as the source for the 4.7-Mev and 7.1-Mev neutrons with bombarding energies of 1.47 and 3.8 Mev, respectively. The gas chamber was 3.8 cm long, 1.3 cm in diameter, and had a beam entrance aperture of 0.6 cm diameter covered by a 0.0001 inch nickel foil. About 0.3 atmos of deuterium gas was used as a target. The detector for the 4.7-Mev neutrons was placed 4 inches from the center of the target; the detector-to-target distance was increased to 12 inches in the experiments with 7.1-Mev neutrons; with such geometry there is a decrease of 50 kev in the energy of the neutrons at the maximum subtended half-angle and a decrease in illumination[13] of 9 percent.

The $T(d,n)He^4$ reaction was used as the source for 12.7-Mev and 14.1-Mev neutrons. The detector was placed 8 inches from the source at 160° to the direction of the incident beam of 675-kev energy to get 12.7-Mev neutrons and at 90° with respect to the 350-kev beam for the 14.1-Mev neutrons.

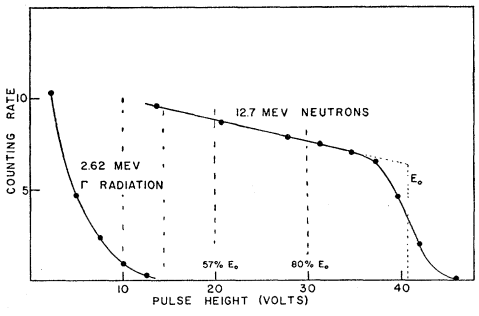

FIG. 2. Pulse-height distribution curve for 12.7-Mev neutrons in 1 cm scintillator and pulse height distribution of γ rays of maximum effective energy.

[12] Willard, Bair, and Kington, Phys. Rev. **90**, 865 (1953); G. A. Jarvis (private communication).

[13] Henkel, Perry, and Smith (private communication).

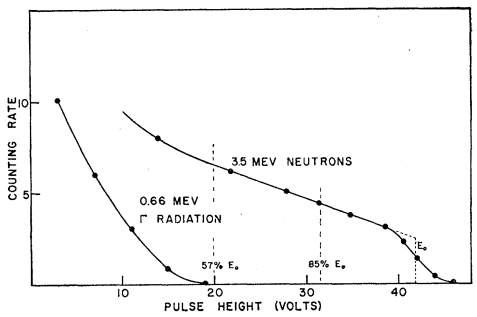

FIG. 3. Pulse height distribution curve for 3.5-Mev neutrons in eight 1.5 mm diameter scintillators and pulse distribution of γ rays of maximum effective energy.

DATA

Figure 2 shows the pulse distribution curve of the neutron detector for 12.7-Mev neutrons and that obtained from the 2.62-Mev γ radiation from a Th C″ source. Figure 3 gives the similar pulse distribution curve which was obtained with 3.5-Mev neutrons and 0.66-Mev γ radiation. The pulse height distribution curve for neutrons is not quite flat, since the pulse height depends on the range of the particle producing the pulse and not its energy.

The pulse-height distribution curves in Figs. 2 and 3 are typical experimental curves which also indicate the relative size of neutron pulses and maximum possible γ-ray pulses. Theoretically the curve should drop off sharply at the upper end as indicated by the E_0 dotted line.

A bias value corresponding to 80% of the energy of the source neutrons was used for the cross-section determination at 12.7 and 14.1 Mev and a value of 85% at 3.5, 4.7, and 7.1 Mev. Data were also obtained with a lower bias in all the experiments. The efficiency of detection as a function of neutron energy was measured for each detector, and the results for the 3.5-Mev neutron detector are shown in Fig. 4 when biased at 85% of the 3.5-Mev energy. The efficiency of detection curves for the other neutron detectors were similar in shape to that given in Fig. 4.

The cross-section data were taken by measuring counting rates with the scatterer in position and removed. The ratio of the counting rate with the scatterer in position to the counting rate without the scatterer is the experimental transmission. Results of these transmissions are given in Table I; each transmission is a mean of 6 to 20 separate experiments. Simultaneously with the 80% or 85% bias, a transmission using a lower bias was taken to find the dependence of the transmission on the choice of bias point.

Figure 5 shows the geometry of the experimental arrangement. The transmission must be corrected because of the uncompensated elastic scattering due (1) to the decreased efficiency of detecting the elastically scattered neutrons of slightly less energy because of energy loss to the struck nucleus, (2) a decrease in the efficiency of detecting neutrons of lower energy from the source which are emitted at an angle ϕ, and (3) the nonuniform illumination of the spherical scatterers.

The detector for neutrons of 3.5, 4.7, and 7.1 Mev was placed at zero degrees with respect to the direction of the accelerator beam on the target and subtended a very small solid angle at the source as indicated in Fig. 5. Thus the neutrons detected when the scatterer was not in position were emitted from the source at essentially zero degrees. When the scatterer was in position, the neutrons which did not reach the detector because of elastic scattering in the portion of the shell directly between the source and detector, at point A in Fig. 5 are assumed to equal (except for small corrections) the number of neutrons elastically scattered towards the detector by the rest of the spherical shell. Such elastically scattered neutrons will not have exactly the same energy as the incident neutrons and, as indicated by Fig. 4, will not have the same probability of being detected. The fraction of the incident neutrons so scattered is $(1-e^{-N\sigma_e})$, where N is the number of nuclei per square centimeter of the scatterer and σ_e is the elastic scattering cross section. The value of σ_e is obtained by subtracting an assumed value of nonelastic scattering cross section σ_n from the total scattering cross section σ_t. When necessary in view of later calculations, the assumed σ_n was revised. The energy lost by a neutron depends on the angle θ through which it is scattered. The number of elastically scattered neutrons as a function of angle of scattering is needed in order to make corrections (1), (2), and (3) listed above.

Angular distributions have been studied with neutrons with energies of 1.0 Mev,[14] 4.1 Mev,[15] and 14 Mev[16] for several elements. Where angular distribution data for an element were not available, the distribution for the element of nearest atomic weight available was used. The 4.1-Mev angular distributions were used for the 3.5-Mev and 4.7-Mev data. The 14-Mev angular distributions were used for the 12.7- and 14.1-Mev data. The 4.1- and 14-Mev angular distributions are similar in that they both show large scattering at small angles. Therefore, since no angular distributions were available near 7 Mev, the effects expected from both 4- and 14-Mev angular distributions were calculated for the 7.1-Mev data and a linear interpolation was made to get the effect expected from 7-Mev angular distributions. The errors introduced by this approximation are quite small except in the case of the very light elements, Be and C, where the error was considered to be too large to make the results very useful. In the case of lead the correction for source energy spread and illumination is 3.7% of the number of elastically scattered neutrons with 4-Mev angular distributions, 1.4% with 14-Mev distributions, and 3.0% for the interpolated value at 7 Mev.

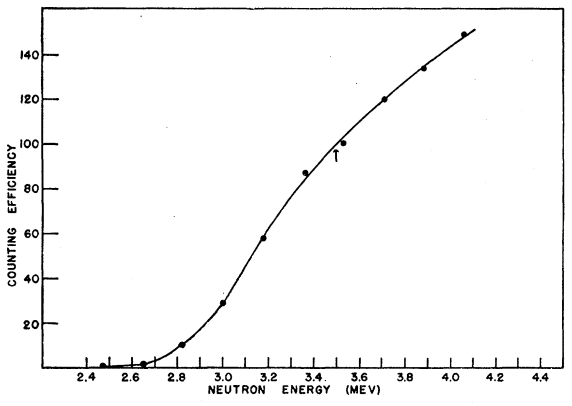

FIG. 4. Relative efficiency as function of neutron energy for detector biased at 85% energy for 3.5-Mev neutrons.

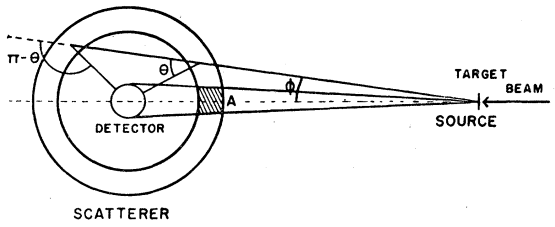

FIG. 5. Diagram showing geometry of experimental arrangement. Neutrons emitted at an angle ϕ to the direction of the beam are elastically scattered through angle θ or $\pi-\theta$ to reach the detector.

The transmissions, corrected for uncompensated elastic scattering are given as T (corrected) in Table I. The difference between the experimental transmission and the corrected transmissions are smaller at the higher energies and with heavier nuclei. Considerable errors may result for light nuclei, especially in the case of Be and C where the corrections are large and the angular distributions do not extend past 90° for 14-Mev neutrons.

The nonelastic cross sections were calculated from an expression derived by Bethe, Beyster, and Carter which takes account of multiple scattering in the shell:

$$(1-T)=(1-T_0)\frac{\sigma_n}{\sigma_n+\sigma_{et}P_m},$$

where T=experimental transmission (corrected), $T_0=e^{-N\sigma_e}$, P_m=escape probability of the neutron, σ_n=nonelastic cross section, σ_e=elastic cross section, σ_{et}=elastic

[14] M. Walt and H. H. Barschall, Phys. Rev. **93**, 1062 (1954).
[15] M. Walt and J. R. Beyster, Phys. Rev. **98**, 677 (1955).
[16] J. H. Coon and R. W. Davis, Phys. Rev. **94**, 786(A) (1954), and private communication.

TABLE I. Summary of experimental results. Tabulated are the experimental transmission T (expt.), the transmissions corrected for elastic scattering effects T (corrected), the calculated nonelastic cross section σ_n, the total scattering cross section σ_t, and the ratio of the nonelastic cross section to the geometrical cross section for each element. The nuclear radius is calculated from the relation $R=1.4\times10^{-13}A^{\frac{1}{3}}$.

Element	Be	C	Al	Ti	Cr	Fe	Ni	Cu	Ag	Sn	Pb	Bi
$N/\text{cm}^2\times10^{22}$	24.0	16.06	12.37	11.38	16.05	16.91	18.18	16.90	11.72	7.40	6.59	5.62
						3.5 Mev						
T (expt.)			0.877	0.832	0.776	0.773	0.717	0.734	0.758	0.845	0.876	0.883
T (corrected)			0.913	0.857	0.813	0.807	0.747	0.767	0.775	0.857	0.891	0.896
σ_n			0.68±0.05	1.24±0.05	1.14±0.04	1.14±0.04	1.48±0.04	1.45±0.04	2.03±0.07	2.00±0.09	1.58±0.07	1.73±0.06
σ_t			2.40	3.67	3.90	3.47	3.35	3.45	4.18	4.28	7.70	7.76
$\sigma_n/\pi(R+\lambda\!\!\!^{-})^2$			0.49	0.70	0.62	0.60	0.76	0.72	0.81	0.73	0.44	0.48
						4.7 Mev						
T (expt.)			0.872	0.828	0.758	0.738	0.703	0.704	0.749	0.826	0.831	0.848
T (corrected)			0.912	0.854	0.797	0.777	0.741	0.737	0.769	0.838	0.851	0.867
σ_n			0.70±0.05	1.32±0.06	1.32±0.03	1.38±0.05	1.54±0.06	1.69±0.04	2.14±0.07	2.33±0.07	2.25±0.07	2.39±0.06
σ_t			2.20	3.40	3.70	3.72	3.55	3.72	4.01	4.00	7.40	7.48
$\sigma_n/\pi(R+\lambda\!\!\!^{-})^2$			0.56	0.81	0.78	0.79	0.87	0.91	0.88	0.92	0.66	0.70
						7.1 Mev						
T (expt.)			0.889	0.848	0.782	0.758	0.743	0.754	0.770	0.844	0.825	0.851
T (corrected)			0.914	0.865	0.809	0.783	0.770	0.779	0.782	0.851	0.833	0.857
σ_n			0.74±0.05	1.21±0.04	1.22±0.04	1.35±0.04	1.33±0.06	1.37±0.05	2.01±0.07	2.12±0.06	2.67±0.07	2.66±0.07
σ_t			1.88	3.18	3.50	3.44	3.60	3.73	4.12	4.08	5.60	5.60
$\sigma_n/\pi(R+\lambda\!\!\!^{-})^2$			0.63	0.83	0.81	0.86	0.84	0.82	0.91	0.92	0.85	0.84
						12.7 Mev						
T (expt.)	0.821	0.892	0.873	0.871	0.810	0.786	0.773	0.768	0.806	0.860	0.842	0.867
T (corrected)	0.871	0.910	0.876	0.873	0.813	0.789	0.776	0.771	0.808	0.861	0.843	0.868
σ_n	0.49±0.08	0.56±0.10	1.06±0.07	1.17±0.06	1.26±0.07	1.36±0.05	1.35±0.05	1.49±0.05	1.75±0.10	1.97±0.09	2.58±0.09	2.47±0.14
σ_t	1.60	1.30	1.69	2.37	2.60	2.67	2.83	3.10	4.41	4.61	5.15	5.05
$\sigma_n/\pi(R+\lambda\!\!\!^{-})^2$	0.92	0.91	1.11	0.91	0.95	0.98	0.96	1.01	0.88	0.94	0.90	0.86
						14.1 Mev						
T (expt.)	0.855	0.899	0.886	0.872	0.802	0.786	0.761	0.777	0.804	0.870	0.843	0.866
T (corrected)	0.909	0.918	0.890	0.873	0.804	0.788	0.763	0.779	0.806	0.871	0.844	0.867
σ_n	0.37±0.08	0.51±0.08	0.91±0.05	1.17±0.04	1.33±0.04	1.38±0.03	1.45±0.05	1.44±0.04	1.78±0.05	1.82±0.06	2.52±0.09	2.50±0.07
σ_t	1.55	1.34	1.73	2.28	2.45	2.60	2.72	2.96	4.34	4.68	5.48	5.46
$\sigma_n/\pi(R+\lambda\!\!\!^{-})^2$	0.72	0.86	0.99	0.94	1.02	1.02	1.05	1.00	0.91	0.88	0.89	0.88

transport cross section $=(\sigma_t-\sigma_n)S$, and

$$S=\frac{\int\sigma_e(\theta)(1-\cos\theta)d\theta}{\int\sigma_e(\theta)d\theta}.$$

To use this formula it is necessary to assume a value of σ_n and use it in the equation. The nonelastic cross section σ_n is subtracted from the known σ_t to determine σ_e. The P_m values have been calculated by Bethe, Beyster, and Carter, and in this experiment had values which extended from 0.65 to 0.84. A trial and error process of successive approximations is necessary to

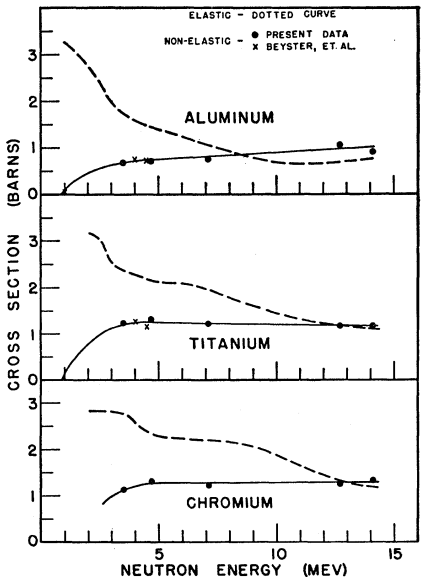

FIG. 6. Nonelastic (solid curve) and elastic (broken curve) cross sections in Al, Ti, and Cr.

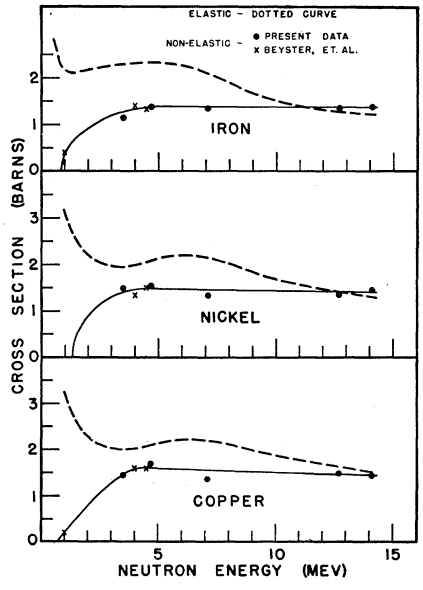

FIG. 7. Nonelastic (solid curve) and elastic (broken curve) cross sections in Fe, Ni, and Cu.

achieve the final result. The calculated nonelastic cross sections σ_n are given in Table I. These cross sections are too small by an amount depending on the number of inelastically scattered neutrons which are still counted by the biased detector. In general this is a small effect and an estimate of its magnitude can be obtained by comparing the cross sections calculated from the data with lower energy bias.

Data taken with 3.5-Mev neutrons and a bias of 57% of the maximum energy instead of 85% gave an average decrease in the cross section of 11% for the elements chromium through bismuth. In most cases the energy of the first excited state is large enough so that inelastically scattered neutrons will have a very low efficiency for being counted when using the 85% bias. For example inelastically scattered neutrons from iron will lose 0.845 Mev or greater energy and will have a relative efficiency for being counted of 2% or less.

With 4.7-Mev neutrons, data were taken with a bias of 70% as well as 85% of the energy. The average decrease in cross section with the 70% bias was 7%, indicating about 7% of the neutrons inelastically scattered to energies between 2.9 and 3.8 Mev. Silver is the only element with energy levels below about 0.6 Mev. The probability of detection of 4.1-Mev neutrons was 50%. Therefore, neutrons exciting levels of 0.6 Mev or less would contribute less than 50% of their cross section to the observed value.

With 12.7-Mev neutrons a bias point corresponding to 57% of the source neutron energy gave cross sections which were an average of only 4% smaller than for the 80% bias. This result indicates that only 4% of the inelastically scattered neutrons have an energy between 7.2 and 10.2 Mev in agreement with the photoplate-experiments of Graves and Rosen that most of the inelastically scattered neutrons have energies less than 5 Mev.

DISCUSSION

The results of the nonelastic cross sections are shown in Figs. 6, 7, 8, and 9. Recent data of Beyster, Henkel, and Nobles[17] at 1.0, 4.0, and 4.5 Mev are also included. Data just published by Graves and Davis[18] with neutrons of energies from 13.5 to 14.7 Mev are in general agreement with our 14.1-Mev data. The elastic scattering cross sections were obtained by subtracting the nonelastic scattering cross section from the best total cross sections that are available.[19–22] There is a marked difference in the variation with energy of the elastic and nonelastic cross sections. This difference is most marked in the case of Ag and Sn where the elastic cross section becomes larger as the energy increases from 5 to 14 Mev. In this same energy interval the nonelastic cross section decreases. In all the elements studied, except for Cu, the nonelastic cross section is greater than the elastic cross section at some particular energy.

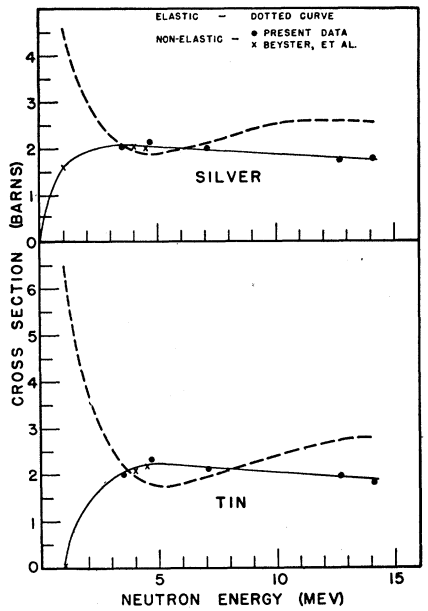

FIG. 8. Nonelastic (solid curve) and elastic (broken curve) cross sections in Ag and Sn.

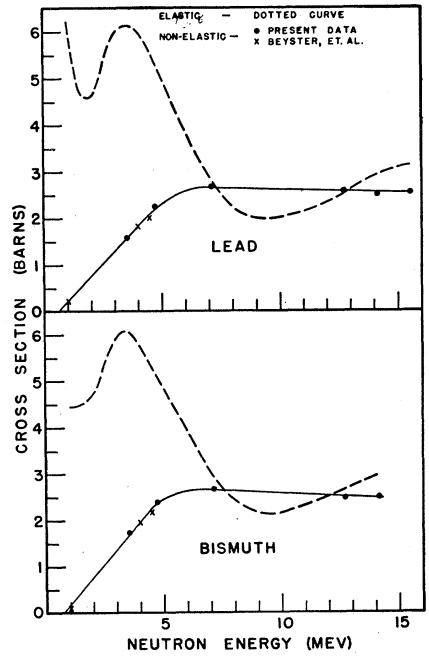

FIG. 9. Nonelastic (solid curve) and elastic (broken curve) cross sections in Pb and Bi.

[17] Beyster, Henkel, and Nobles, Phys. Rev. **97**, 563 (1955).
[18] E. R. Graves and R. W. Davis, Phys. Rev. **97**, 1205 (1955).
[19] N. Nereson and S. Darden, Phys. Rev. **89**, 775 (1953); Phys. Rev. **94**, 1678 (1954); and private communication.
[20] *Neutron Cross Sections*, U. S. Atomic Energy Commission Report AECU 2040 and 3 supplements (Technical Information Division, Department of Commerce, Washington, D. C., 1952).
[21] Bonner, Alba, Fernandez, and Mazari, Phys. Rev. **97**, 985 (1955).
[22] McCrary, Taylor, and Bonner (unpublished data on Cr).

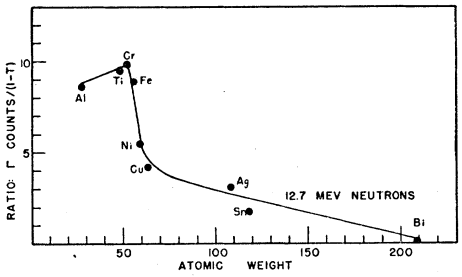

FIG. 10. Relative number of observed γ rays with energies greater than 3 Mev from inelastic scattering of 12.7-Mev neutrons.

The shape characteristics of the elastic scattering cross sections appear to vary smoothly with atomic weight. These variations of elastic scattering cross sections with atomic weight appear to fit qualitatively the predictions by the Weisskopf "cloudy crystal ball" model,[23] where the location of wide resonances appears as a function of the nuclear radius. In this model the nuclear potential is taken as a complex square well of the form $V=V_0(r)(1+i\zeta)$, where ζ is some real number which gives the absorption necessary to account for the formation of a compound nucleus. Feshbach, Porter, and Weisskopf[22] fitted the total cross sections up to about 3 Mev with this model using a ζ equal to 0.03. The large nonelastic cross sections obtained in the present experiments require a larger ζ at higher energies.

Comparison of the measured nonelastic cross section to the geometrical cross section is shown in Table I. The nuclear radius R was calculated from the relation: $R=1.4\times10^{-13}A^{\frac{1}{3}}$. The nonelastic cross sections for 12.7- and 14.1-Mev neutrons are very nearly equal to the geometrical cross sections: $\pi(R+\lambda\!\!\!^{-})^2$. At 4.7 Mev the nonelastic cross sections are still between 0.8 and 0.9 of the geometrical cross section in Cr, Fe, Ni, Cu, Ag, and Sn; in the nuclei Pb and Bi, which have closed shells and a lower density of energy levels, the cross sections are only 0.66 and 0.70 of the geometrical.

Comparison of nonelastic cross sections and elastic cross sections at 12 to 14 Mev indicates that there is an interference of waves entering the nucleus, suffering only a phase change without stronger interaction, and then interfering with the incident waves. At 14.1 Mev for Al, Cr, Fe, and Ni, the ratio $\sigma_n/\pi(R+\lambda\!\!\!^{-})^2$ is greater than one. At this energy these elements have an elastic cross section which is less than the nonelastic cross section. Similarly, it is noticed that for Pb and Bi at 14 Mev the ratio $\sigma_n/\pi(R+\lambda\!\!\!^{-})^2$ is particularly low, and the elastic cross section is greater than the nonelastic cross section. Both these results can be explained by interference effects.

[23] Feshbach, Porter, and Weisskopf, Phys. Rev. **90**, 166 (1953); Feshbach, Porter, and Weisskopf, Phys. Rev. **96**, 448 (1954).

γ RADIATION FROM INELASTIC SCATTERING OF 12.7-MEV NEUTRONS

When the 12.7-Mev data were taken, one of the channels of the pulse-height analyzer was set to count pulses with heights between 10 and 14 volts, as indicated by dotted lines on Fig. 2. Some of these pulses were produced by γ rays with an energy greater than 3 Mev. This channel corresponded to the largest pulses from neutrons with energies of from 5.2 to 6.3 Mev. Since the results of Graves and Rosen show that there are very few inelastically scattered neutrons of this energy, any increase in the counts in this channel with the sphere in position are due largely to γ radiation produced in the scatterer. There are more counts in this channel for many elements with the scatterer on than with the scatterer off. This increase in counting above the expected neutron counts was attributed to γ rays produced by the inelastic scattering in the sphere. The ratio of γ counts to the neutron absorption $(1-T)$ is plotted as a function of atomic weight in Fig. 10. The fact that more high-energy γ rays are observed from lighter elements than for the heavier ones is explained by the fact that $(n,2n)$ reactions have higher cross sections for heavier elements and comprise a greater portion of the nonelastic cross section than for the lighter elements. This follows because in an $(n,2n)$ reaction, γ radiation above 3 Mev is not expected. The $(n,2n)$ cross section for 12.7 Mev neutrons is not known for most of the elements studied. The results with Bi indicate that nearly all the nonelastic cross section of 2.5 barns is due to the $(n,2n)$ cross section. The $(n,2n)$ reaction is energetically impossible in aluminum and so this cross section must be zero. The experimental results indicate a small cross section for $(n,2n)$ reactions in Ti, Cr, and Fe, which all give about the same amount of γ radiation as aluminum. Less γ radiation is observed from Ni, Cu, Ag, and Sn, and indicates a considerable cross section for the $(n,2n)$ reactions in these elements for 12.7-Mev neutrons.